SNAME Maritime Convention 2020-A Virtual Event

29 September- 2 October Copyright © 2020 Society of Naval Architects and Marine Engineers (SNAME) www.sname.org



Improving the Visibility of Underwater Video in Turbid Aqueous Environments

Sanat Upadhyay¹ (V), Manos Papadakis² (M)

- 1. Lolaark LLC, Houston, TX, USA
- 2. Department of Mathematics, University of Houston, USA

Water turbidity is a frequent impediment for achieving satisfactory imaging clarity in underwater video and inhibits the extraction of information concerning the condition of submerged structures. Ports, rivers, lakes and inland waterways are notoriously difficult spots for camera inspections, in particular for hull inspections in lieu of drydocking. This complex problem motivated us to study methods to extract a cleaner image /video footage from the acquired one. The purpose of this paper is to describe a novel mathematical model for the degradation of images due underwater turbidity caused by suspended silt particulates and algae organisms and to propose methods to improve image and video clarity using multiscale non-linear transforms.

KEY WORDS: Algorithms, Underwater, Camera Inspections, Turbidity, Dehazing

INTRODUCTION

Water affects light propagation due to scattering, which is increased by suspended solid particles in the water. Light absorption is one way this effect manifests. Turbidity is an optical determination of the level of water clarity and is caused by variety non-soluble particles, e.g. clay, sand, silt, or algae. Suspended particulates are those having diameter larger than 2µm. Anything smaller is considered soluble. In average, salt water environments have lower turbidity levels than freshwater ones. In this work, we discuss some ideas on how to model image formation in aqueous environments and we propose a new method on how to restore clarity of still photos and video (*live feed or saved in a file*). We also discuss what our method can extract from a given image and possible ways of improving clarity restorations in the future.

Underwater Image Formation

First, we begin with a description of how images are formed, ideally, in vacuum, or in clear atmospheric conditions. The key principle is derived from Lambert: the image f is expressed as

$$f = Luminance(\sigma) \times Reflectance(R)$$
 (1)

where the luminance σ depends on the incident light. Luminance can also account for the lower illumination a shadow may cast on an object. The reflectance accounts for the portion of the luminous energy that can be reflected back from the object, hence it contains all the necessary information for the shape of an objects and its boundaries with other objects, crack lines and all of the necessary structural information we want to know. The problem of interest is to recover R without knowing σ . When adequate light from a

scene reaches the sensor we conventionally have R=f. If very low luminous energy is emitted back from the scene, then recovering R from f may become impossible. Recovering or better say approximating R in some sense, is the goal of Illumination Neutralization algorithms, a term the authors were first to coin in (Upadhyay and Papadakis 2019). By Illumination Neutralization, we mean the process to derive a surrogate R_s of R from f with the following properties:

- R_s contains all the edges of R and does not contain artificial edges.
- Smooth areas of R are preserved in R_s
- Edges in R_s are spatially organized in the same way as in R in order to preserve all shapes in R.

In (Upadhyay and Papadakis 2019) we provide a mathematical definition for R_s so we refrain from giving more details here. As we argue therein, from a given f we can extract more than one surrogate of R which circumvents the problem of extracting the reflectance from a given image which is not a well-posed problem since luminance is also unknown. Numerous contributions have been made claiming to solve (1) but many of them lack rigor and deliver a surrogate of R while they claim that they extract R. The need to avoid such mathematically non-rigorous approaches leads us to introduce Illumination Neutralization.

Image formation in marine environments differs from the model of Eq. (1) because light is scattered on water molecules and quite often on NaCl molecules as well. In simple terms those molecules function as microscopic reflectors causing incident light to be dispersed in multiple directions and also back to the direction of the camera. Apparently light rays scattered by one molecule will be scattered multiple times, but these multiple scatterings are ignored. To account for the cumulative effect of these scatterings Jaffe and McGlamery (McGlamery 1980) (Jaffe 1990) suggest that image acquisition in underwater is governed by:

$$f(x) = \sigma(x)R(x) + A(1 - \sigma(x))$$
(2)

where, σ is a light absorption function and A models the ambient illumination from the sun. The same model also postulates that

$$\sigma(x) = Ae^{(-Kd(x))} \tag{3}$$

where d(x) is the distance of an object inside the water from the point x of the camera sensor plane and K is constant. The object also reflects light back to the camera. This a widely accepted model for image formation in non-turbid aqueous environments. Two interesting points arise when comparing this model to Eq. (1): First, the term of the sum in (2) is a special case of the righthand side (RHS) of (1) while here we have an explicit form for the luminance assuming we know d; second, the second term in the sum models haze. The significance of the model is that we have an additional term to account for when solving for R. When we use underwater lights in non-turbid aquatic environments, we can essentially ignore the second term if the image f captures a scene with objects not far from the camera. In this case, A will be the light intensity of the camera. The Jaffe and McGlamery model inspired us to propose a model for image formation in turbid aquatic environments utilizing again two terms as in (2). Our motive to explore underwater image formation in the presence of turbidity is the need to develop training sets for deep neural networks tuned for the detection of structural problems during camera inspections. Obtaining real training sets is a rather difficult task, but using images obtained not in aqueous environments is an easier task. Then, if we can simulate turbidity then we can possible create training sets for the AI-detection of certain defects underwater.

Underwater Image formation when turbidity is present. Here we assume that light only comes from the direction of the camera. We ignore ambient sun light because it is either highly attenuated or non-existent (e.g. in a ballast tank or under ice). Then, we must have that an image f is given by

$$f(x) = \sigma(x)R(x)(1-q(x)) + A_{cam} q(x)$$
(4)

where q is a "function" accounting for the interaction of the artificial light with intensity A_{cam} . The "function" q is non-deterministic. In fact, we postulate that q is a random field, which is the analogue of a random process in two dimensions. As we see both summands in the RHS of Eq. (4) are coupled as in the Jaffe and McGlamery model due to the presence of q. This does not allow us to treat the second term in the sum as noise. So recovering R from f is a lot more complicated problem because f is the sum of two images one of which, $A_{cam} q$, is a random field and a more special type referred to as texture. This type of texture is stochastic or in simple words we mean that it does not have a specific pattern as for instance a brick wall has. Even in this more complicated situation we want to extract a surrogate of R. To solve this problem we argue that it will be important first, to model q.

The rest of this work discusses a plausible model for q and partial solution for the extraction of a surrogate of R under certain

conditions using methods proposed in (Upadhyay and Papadakis 2019) (Upadhyay, Mitsakos and Papadakis 2018).

METHODS

Modeling q. There are two visible properties of textures or intensity patterns that is created by turbidity in natural sub-aquatic environments.

- 1. The back scattered light appears to be reflected from suspended particles that are randomly distributed. The average intensities across the image is mostly uniform for uniform illuminations.
- 2. These suspended particles appear at many scales. At a fixed distance from the camera, smaller particles are more densely distributed than larger ones. However, larger particles at greater distance from the camera appears similar to smaller particles close to the camera.

These two properties suggest that we should model q using stochastic texture that also has a self-similar statistics across different scales. That is, textures at courser scales show same statistical behavior as those in finer scales. These two properties can together be addressed using a family of stochastic texture called *fractional Brownian motion* (fBm) random fields. Our larger goal is to simulate turbidity across many 2D planes at multiple depths in the field of view, and then find the cumulative effect of their superimposition. However, we are going to limit our scope of research to only one such plane in this article.

Ordinary Brownian motion. An ordinary Brownian motion also known as a Wiener process is a continuous-time stochastic process W(t) for $t \ge 0$ with W(0) = 0 and such that the increment W(t)-W(s) has normal distribution with mean 0 and variance t-s for any $0 \le s < t$, and increments for non-overlapping time intervals are independent (Karatzas 1997).

Fractional Brownian motion. The term fractional Brownian motion was first introduced by Mandelbrot and van Ness in 1968. They used fBm as a special category of Gaussian stochastic processes in one dimension, which followed certain specialized properties. These models were later generalized into higher dimensions, and we are going to adopt a two dimensional version of fBm models for simulation of turbidity at a given plane perpendicular to the line of sight of the camera (or the principle axis of the lens).

It is simpler to understand the underlying principal of fBm by looking at its definition in one dimension, which is given by an integral:

$$B_H(t) = \int_{-\infty}^{+\infty} [K_H(t-s) - K_H(-s)] dB(s)$$
 (5)

where,
$$0 \le H \le 1$$
,
 $K_H(t) = \frac{t^{H-0.5}}{\Gamma(H+0.5)}$ (6)

for $t \ge 0$ and $K_H(t) = 0$ for t < 0, and $\{B(s)\}_s$ is ordinary Brownian motion (i.e., the integration of a white Gaussian

process) (Abry and Sellan 1996). Thus a fractional Brownian motion is a moving average of an ordinary Brownian motion, weighted over a Kernel. Fourier transform of $B_H(t)$ shows that it does not have any dominant frequency, rather the frequencies are spread across the spectrum in a way that each frequency to the power spectrum is nearly inversely proportional to the frequency. In addition, the increments of fBm are statistically self-similar, that is, $B_H(t + \Delta t) - B_H(t)$ and $h^{-H}[B_H(t + h\Delta t) - B_H(t)]$ have the same distribution functions. The positive quantity H is called the Hurst parameter and works as the self- similarity parameter. Higher dimensional extensions to fBm follow the same properties, making them suitable for our modeling (Fournier, Fussel and Carpenter 1982).

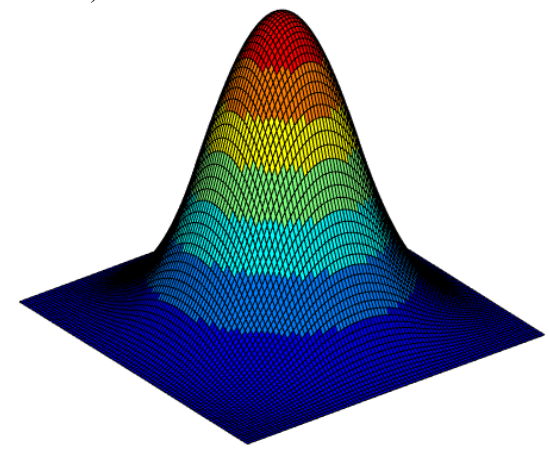


Figure 1. B-Spline averaging filter used to generate \mathbf{q} in the second term of Equation (4). The texture \mathbf{X} is the physical barrier of suspended particulates and \mathbf{q} is the image of \mathbf{X} captured by the camera. To arrive at step 6 of the turbidity texture generating algorithm we use this filter as an averaging kernel before lowering the resolution as in step 3.

Generating fBm fields using midpoint displacement algorithm.

The midpoint displacement algorithm is a method to generate an intensity map by assigning a value to each of the four corners of a rectangle, and then subdividing the rectangle and each resulting child into four smaller rectangles, whose value at the subdivided corners are the average value between the corners of the parent rectangle perturbed by a randomly generated Gaussian white noise (Brouste, Istas and Lambert-Lacroix 2007). The Matlab implementation we used to derive the simulations of the fBm are due to Meg Noah (Meg n.d.).

Proposed numerical scheme to generate turbidity.

We assume that the sensor of our digital camera records images as rectangular matrices of size $M \times N$. Let us recall that the field of view of this camera is pyramidal in shape when we observe the same in 3D. That is, texture matrices of larger dimensions gets projected to size $M \times N$ for planes far away from the camera. For the sake of simplicity, we choose only those grid points along the depth where matrices of size $(2^{j}M)x(2^{j}N)$ for some $j \ge 0$ gets

projected to $M \times N$. We adopt the following algorithm to generate a monoscale texture q.

- 1. Generate 2D fBm stochastic texture X of size $(2^{j}M)x(2^{j}N)$ using midpoint displacement algorithm. The values of X scaled to lie between [0,1]. This is a monoscale (all particulates have the same size regardless of their distance from the camera).
- 2. Convolve *X* with 2D low pass analysis filter that is a B-spline of order 3. These kernels are symmetric and smooth, hence good for interpolations. A 3D graph of the low pass filter is attached in Figure 1.
- 3. Downsample X by eliminating alternate rows and columns to obtain X. This delivers a matrix of size $(2^{(j-1)}M)x(2^{(j-1)}N)$.
- 4. Set X = X'
- 5. Iterate steps (2) to (4) *j* times in order to arrive at the texture *X* of size M x N matching the resolution of our camera.
- 6. The matrix q = 1-X is the image of water turbidity captured by the camera (Figs. 4,5). The brighter the image the more opaque water is due to a higher concentration of suspended particulates.

The particles present in this texture are all of the same size,

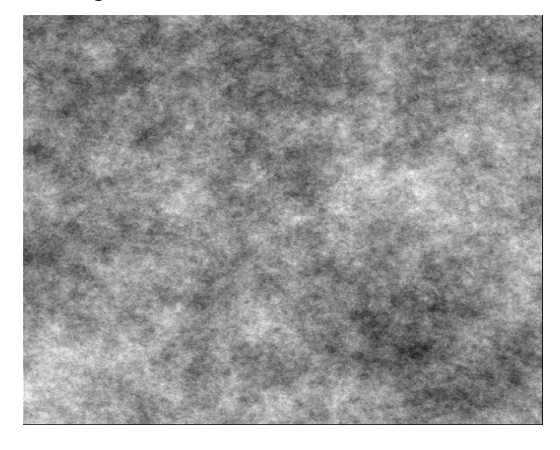


Figure 4 Example of a turbidity image obtained with algorithm above. The brighter areas of the image indicate higher concentration of particulates reflecting more light back to the camera. This is an image of the texture **q**.

because our present construction makes that assumption. Yet they generate a range of intensities because they do not reflect back all the light hitting them. We assume these particles to be spherical in shape, and hence light may bounce off in a direction depending on the surface normal at the point of incident. It is extremely difficult model the net incident light by studying reflected light at the particle level. So, we adopt the strategy to model the cumulative effect of lights coming to the sensor after factoring in the possibility that some light may be lost because it does not propagate towards the sensor.

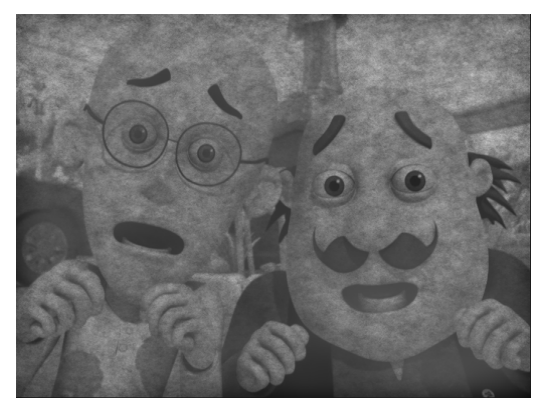
Finally, we are ready to model Equation (4), where we superimpose the turbidity on an actual target image in the background. Our results here represent work in progress. At this stage we model turbidity only for gray-scale images. Modeling turbidity for color images is a quite more complex problem that will be the objective of our future study.

We assume that out some of the incident light is not reflected back because it is obstructed by suspended particulates. The light that is reflected back due to turbidity is scattered across every direction but our interest lies only in that component which is directed towards the sensor. We find experimentally, that this cumulative reflection can be approximated by convolving 1-q with a normal radial, distribution density function in 2D with std=8 (pixels) along any axis.

Next, we present a few examples to demonstrate the efficacy of this algorithm to generate the effect of turbidity on some natural images of objects photographed in air. The reader may notice that a certain lack of clarity similar to what is observed in turbid water is evident in the images created by monoscale simulated turbidity. We do not claim that we have fully simulated turbidity. This will require a refinement of the previous algorithm to incorporate several sizes of particles. Here we only report partial results of our ongoing research project to model the effects of suspended particulates in underwater image formation.

We assume that approximately 40% of light gets obstructed in the medium, hence $\sigma(x)=0.6$. Four images are chosen to represent R(x) in Equation (4). The first image is that of Indian cartoon characters Motu and Patlu. A cartoon image is always a good first test case. They allow us to observe the effect of an image analysis process on a simple example because cartoons consists of very smooth surfaces combined with very sharp edges. Notice that the two characters are close up. When one observes the effects of captured in simulated turbidity, that the captured image f then notice that the background details, those that would be far from the camera, are not discernible anymore as it happens in turbid water.

We observe that turbidity images generated by our process appear to show particulates of same size spread across the image in a random manner. Very high frequencies, ω , are not lost in the turbidity. This agrees with the theoretical understanding that fractional Brownian motion is among the family of (I/ω) -noise, meaning that the frequency spectrum of fBm texture has a decay of I/ω , making higher frequencies very weak in the monoscale texture. Currently, we work on developing a more general model for \boldsymbol{q} using multiscale methods, which will allow us to incorporate



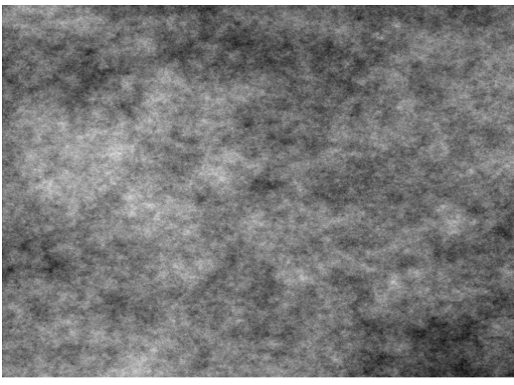




Figure 5 Motlu and Patlu in the bottom. This image is used to generate the top panel using Eq. (3) and the turbidity image in the middle panel.

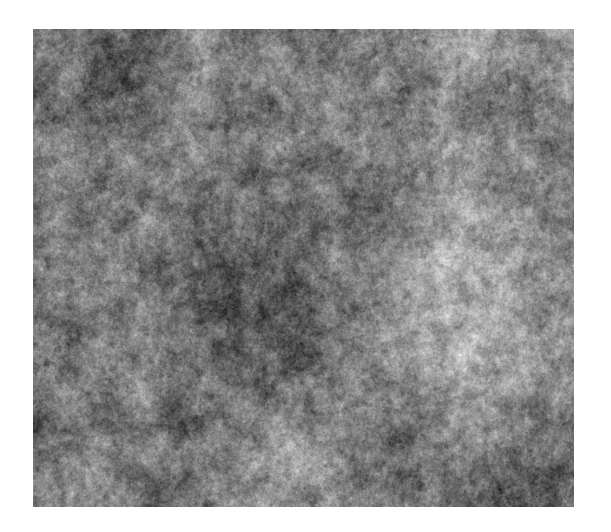






Figure 6 Top panel is an example of a texture q applied again via Eq. (4) to the original shown in the middle panel to derive the hazy output f. The mid-panel photo is taken out of water and shows part of a dock and a umbilical tube.

particles of many different sizes and will have a slower decay of frequencies in their Fourier spectrum.

Improving the Visibility of Underwater Video in Turbid Aqueous Environments Manos Papadakis

Illumination Neutralization

In this section we illustrate a method to extract a surrogate of the reflectance R from f. In (Upadhyay and Papadakis 2019) we rigorously define illumination neutralization and we show two examples of operators performing this task under the assumption that the imaging regime is governed by the Lambertian model of Eq. (1). One note before we proceed will promote better understanding: we often refer to scales as opposed to frequencies. The term scales refers to frequency bands determined by upper and lower bounds that are powers of two and have some orientation, horizontal, vertical, diagonal, or some other intermediate. The higher the powers of two the higher the scale is, pretty much as octaves in music.

We do not yet have a rigorous mathematical proof that neutralization operators will work in the presence of turbidity, but as it happens with numerous algorithms, one example of neutralization operator appears to improve image clarity and definition even in turbid environments governed by Eq. (4). Exploring the mathematics of illumination neutralization under

the regime of Eq. (4) is one of the main objectives of our future research. In this article we will skip all of the mathematical details of this class of operators. We will only describe here how an illumination normalization operator works. There are two key ideas in devising such an operator. The crucial information in reflectance is concentrated on edges which describe shapes.

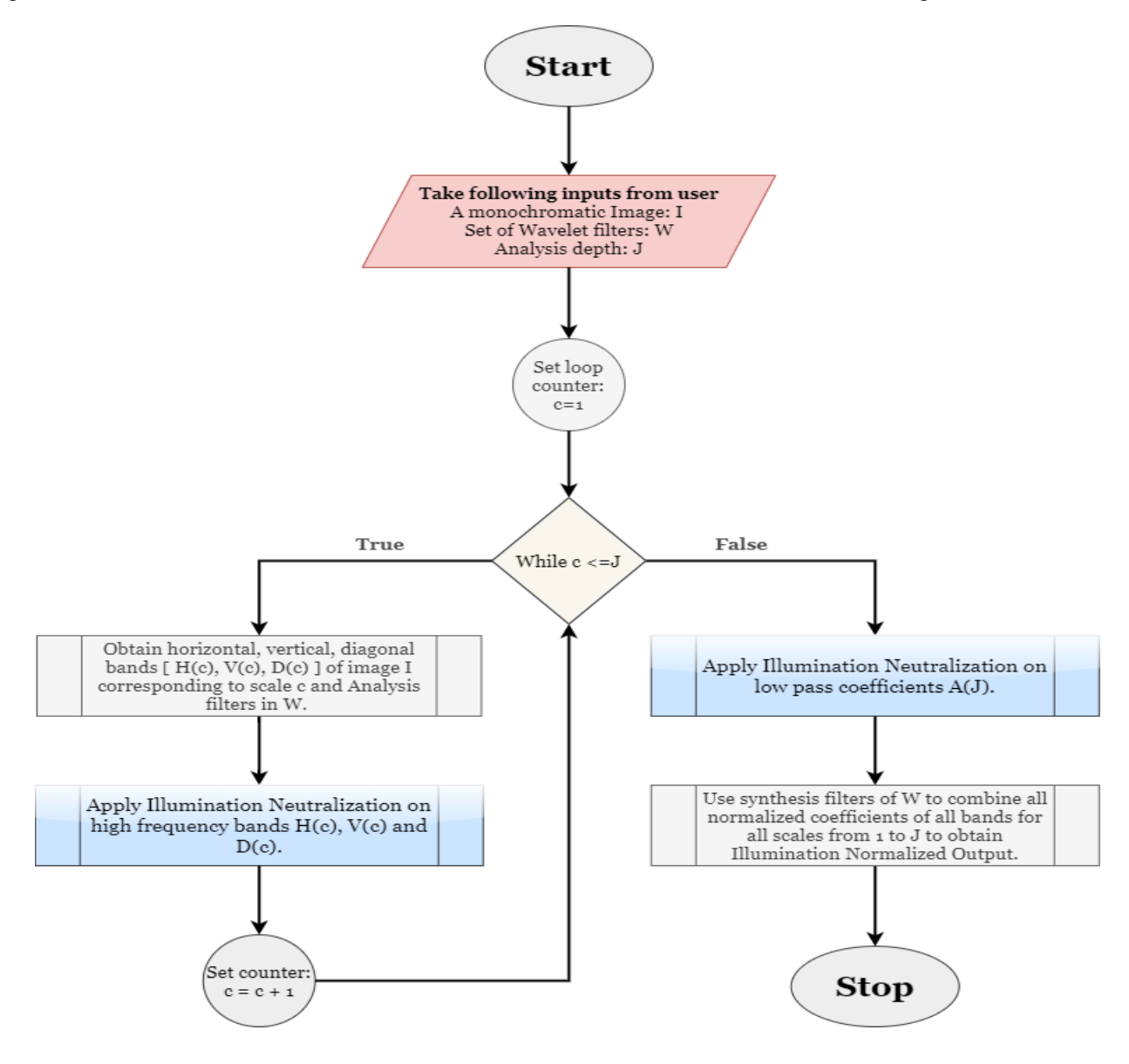


Figure 7 Flow chart of the Illumination Neutralization operator we use for video and photo clarity enhancements. The formulation of this operator is in (Upadhyay and Papadakis 2019). The illumination neutralization applied to each band can be tuned for each band, high and low frequency for better performance for each imaging regime. Further details regarding the steps described in the two blue boxes can be found in (Upadhyay and Papadakis 2019); all rights reserved.

Curvature of smooth surfaces is the other main ingredient of reflectance. Depending on the intensity of illumination, curvatures of smooth surfaces may be preserved in the captured image, but as it happens with human vision, edges are more resilient and many of them, not all, survive poor illumination. An Illumination Neutralization operator restores the original definition of edges under certain circumstances and delivers a surrogate image containing the information we described in the introduction. In (Upadhyay and Papadakis 2019) we prove that the surrogate image we extract by applying an illumination neutralization operator to an image with luminance σ is approximately equal to the surrogate image we would obtain with full intensity luminance $\sigma=1$. We remark that in the latter case f=R. So the surrogate image we will extract from f is not going to be equal to R but it will have all the useful information of R we need to recover from the camera input *f*, that is shape information. In (Upadhyay and Papadakis 2019) we argue there can be more than one illumination neutralization operator and that surrogate images resulting from the same scene contain all edges in the reflectance of the scene. For each scene we have only one reflectance because reflectance exclusively depends on their shape and relative position in the scene. In (Upadhyay and Papadakis 2019) we prove that under certain low or high intensity illuminations σ the resulting surrogate images have very small difference from the surrogate image a Illumination Neutralization operator generates when $\sigma=1$, as long as σ is uniformly smooth and the parameters for the definition the Illumination Neutralization operator are not changed. In summary, we prove that under most illumination conditions from a unique scene we extract an approximate illumination invariant image, the surrogate of R when illumination if full and uniform ($\sigma=1$).

Nonetheless, the mathematical assumptions we make, intentionally ignore one key factor: When illumination σ is very low on certain patches of an image then less energy hits the sensor is not able to capture a part of the edge at that patch. This complete loss of input information sometimes can be recovered by using directional representations, which use filters that have aspect ratios far from 1, come in a variety of orientations, and can align with edges. These representations are sparse, in the sense that they use only a few local "building blocks" (finite elements are one example of such blocks) to locally express an image as a linear combination. In aggregate these "building blocks" are not linearly independent. This redundancy affords representations with directional "building blocks" that are sensitive to edges and resilient to the presence of adversities such as noise or the "veil" of turbidity. Nonetheless, a discussion of such filters is beyond the scope of this paper. The filters we use in our operators tend to align with edges close to horizontal and vertical directions. Moreover, edges manifest in various scales: Consider hair and lip lines for instance. The latter are more pronounced than the former, hence they are captured in intermediate scales, while the former are captured only in high scales. Fine or thin edges are akin to high scales while thicker and sharper (higher gradient) edges appear in a range of scales from intermediate to high. This analysis applies only to the model of Eq. (1).

Turbidity adds another layer of complexity because we have two images superimposed on one another as Eq. (4) shows. In this imaging regime, we can assume that illumination is adequate, so low values alone are not the problem. In fact, as Eq. (4) suggests, that the turbidity generated texture q first blocks the light energy emanating from an object in the scene to reach the camera, while at exactly the same spot what is blocked is adversely compensated by a significant amount of energy emanating now from the scattered light on the very turbidity particulates blocking the light from the object to reach the camera. To improve image clarity first we need to undo the superimposition of the desirable image

$$\sigma(x)R(x)(1-q(x)) \tag{7}$$

from the undesirable $A_{cam}q(x)$. In the former term the product $\sigma(x)(1-q(x))$ can be roughly treated as a form of luminance (Upadhyay, Mitsakos and Papadakis 2018). Currently, the mathematical assumptions we use in (Upadhyay and Papadakis 2019) do not even cover this case, but our illumination neutralization method truly enhances the clarity of images acquired in underwater turbid environments, while the parsing of information in multiscale seems to significantly attenuate the contribution of $A_{cam}q(x)$ in the processed image (Fig. 9). This analysis suggests that moving forward the use of multiscale transforms with directional sensitivity in several select orientations can further enhance the surrogate image illumination neutralization extracts from $\sigma(x)R(x)(1-q(x))$ because this component contains edge information, while $A_{cam}q(x)$ does not have local dominant directional components due to its stochastic nature. This short analysis also provides some initial explanations why it is not expected to see algorithms based on mere local intensity value statistics, e.g. Histogram equalization, Local Histogram Equalization, (Zuiderveld 1994) and references therein, to help improve clarity of images as those algorithms rely on local statistics of the sum of the two previously mentioned terms. This discussion is also the motive for us to try to model image formation in turbid aqueous environments. This type of rigorous approach will help us understand the mathematical intricacies of image clarity restoration under such conditions. Closing, we remark that the turbidity simulation method we presented can be utilized to simulate other visibility inhibiting conditions, e.g. smoke. The reader may have already noticed that our turbidity images look more like smoke. We believe that this is may be happening because in the simulations we used in this paper are monoscale fractional Brownian motions.

EXPERIMENTS

There are a few commercially available products for real-time underwater video clarity restoration. Most are based on various forms of histogram equalization. When simple haze is the visibility compromising factor: all of them appear to give comparably good results with often faithful color adjustments, e.g. (Arici, Dikbas and Altunbasak 2009) (Chiang and Chen 2011) (Li, et al. 2016) (Zhang, et al. 2017) (Celik and Tjahjadi 2011) (Schettini and Corchs 2010) (Lu, et al. 2016). On the other hand, when serious turbidity is present their results appear to be looking more like the original hazy input. The most advanced method for

histogram equalization is the Contrast-Limited Adaptive Histogram Equalization (CLAHE) (Zuiderveld 1994) that also has some "multiscale" variants, in the sense that the more than one window sizes are used to improve local contrast by adjusting the local intensity histogram. More recently, various AI-based systems have also been proposed (Ding, et al. 2019) but do not seem to give better results than HE-based methods, primarily because AI-systems require training and their training requires enormous amounts of data. On the other hand, the manifestation of turbidity is complex and underwater environments have significant variations, limiting the ability of such systems to overcome training constraints. Essentially, turbidity acts as a strong adverse input that a HE-based system is not designed to handle in order to capture reflectance. Demo results of such systems are also obtained under plain haze and not in the presence of serious concentrations of suspended particulates. Using the Illumination Neutralization method, we propose in this paper we significantly restore clarity in underwater images captured in even in inland turbid water conditions, such as lakes, and show that Illumination Neutralization gives better results than HE-based systems in such adverse conditions. At the deployable software level video footage clarity restoration can be executed literally in real-time at 24fps or offline on saved photos or video. Under such conditions all space domain statistics-based methods are not expected to work equally well, because, as we argue in the first subsection of our methods presentation, images acquired in turbid conditions are the superposition of two images, one from the object and another one from light scattering on turbidity particulates. Unlike multiscale methods space domain statisticsbased algorithms cannot parse these two superimposed images. Only when light scattering on water and salt molecules are the only two factors contributing to haze, and silt particulates are present in very low concentrations, then CLAHE and Illumination Neutralization will give results that are hardly distinguishable. We compare outputs of both methods in Figs. 10, right column and 11). The CLAHE algorithm we used for the experiments we report is implemented by the MATLAB command *adapthisteg(.)* with the default parameters.

Only one Illumination Neutralization Operator is currently implemented in the commercially available software suite ALSvisionTM. This software works both in real-time and offline. Unless otherwise stated, all images clarified using illumination neutralization algorithm that are shown here were produced with ALSvision OfflineTM. One final significant note is warranted before closing this section: Turbidity particulates scatter luminous energy (Jaffe 1990). Consequently, it is crucial to have enough of it and to avoid pointy light sources. Led light beams need to be spread so their beams are widened to facilitate as uniform as possible illumination of the surveyed region. Also keeping the lights at some distance from the camera and in symmetric positions around it and at an angle relative to the camera axis will give best results as the close up particulates will not be illuminated and a smaller percentage of light scattered on particulates be directly reflected to the camera. Our experimentation shows that point sources also tend to flare up the different layers of turbidity as if someone views a lit light source behind steam billowing over a tea pot.

CONCLUSIONS

We presented a novel, multiscale non-linear method implemented on a GPU that restores the clarity of video footage and photos when water turbidity, inland or offshore is high. Our methods have the potential to enable vessel camera inspections in ports and inland waters to a much greater degree than currently allowable. This can save downtime in marine operations, costs, operational time savings and reduce risk since inspections in weather sheltered locations are always preferred. Furthermore, the proposed methods can be applied to pipeline and other fixed installation camera inspections in turbid aqueous environments such as lakes and rivers. Our approach is based on deriving a surrogate image of a scene containing all useful shape information. We refer to this process as illumination neutralization. We also presented some novel ideas for a model of image formation in turbid underwater environments. We also provided some initial evidence about the validity of our model. Understanding mathematically image formation in turbid water will enable researchers to improve the accuracy of the extracted surrogate images of reflectance and even develop relevant Deep Neural Network models to advance this task and also to enable object detection, corrosion identification and automated classification of structures and marine life because it will enable the massive enrichment of training sets by overlaving simulated turbidity on images containing objects from the classes of interest acquired even outside of water.

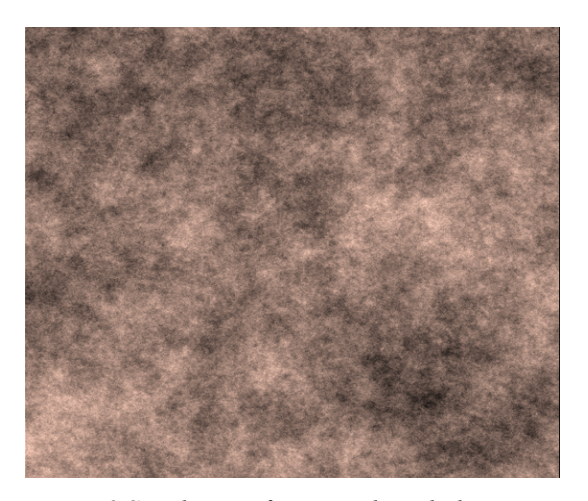


Figure 8 Simulation of monoscale turbidity generated by brown silt shown as a colored image. Here the hue is a Gaussian centered at red with small standard deviation just to render a brown color

For the near future, we plan to carry out a comprehensive study of the proposed turbidity model we launched with this paper. So far, we only looked at monochromatic images and simple textures is generated only for fine grained particulates of one scale only. Although, our results show that we move to the right direction we are not there yet. The aims of our future work are:

- 1. Simulate turbidity generated from particulates of different sizes. Natural turbidity is a combination of many different substances, each of different size and color. The visibility is often dominated by size of particle and distance form camera. This property of a particulate is described by its scale. Particles existing in coarse scales often block the view of other particles at finer scales. We want to create a multiscale model that respects this hierarchy in an effort to develop more realistic examples of turbidity textures q. This first step will be restricted to grayscale images only.
- 2. Next, we will model turbidity for color images. Natural turbidity is colored due to various factors such as color of the suspended particulates the algae or chemical pollutants, etc. It is possible to generate colored texture by extending the process to the color channels of RGB images. An example is shown below in Figure (9).

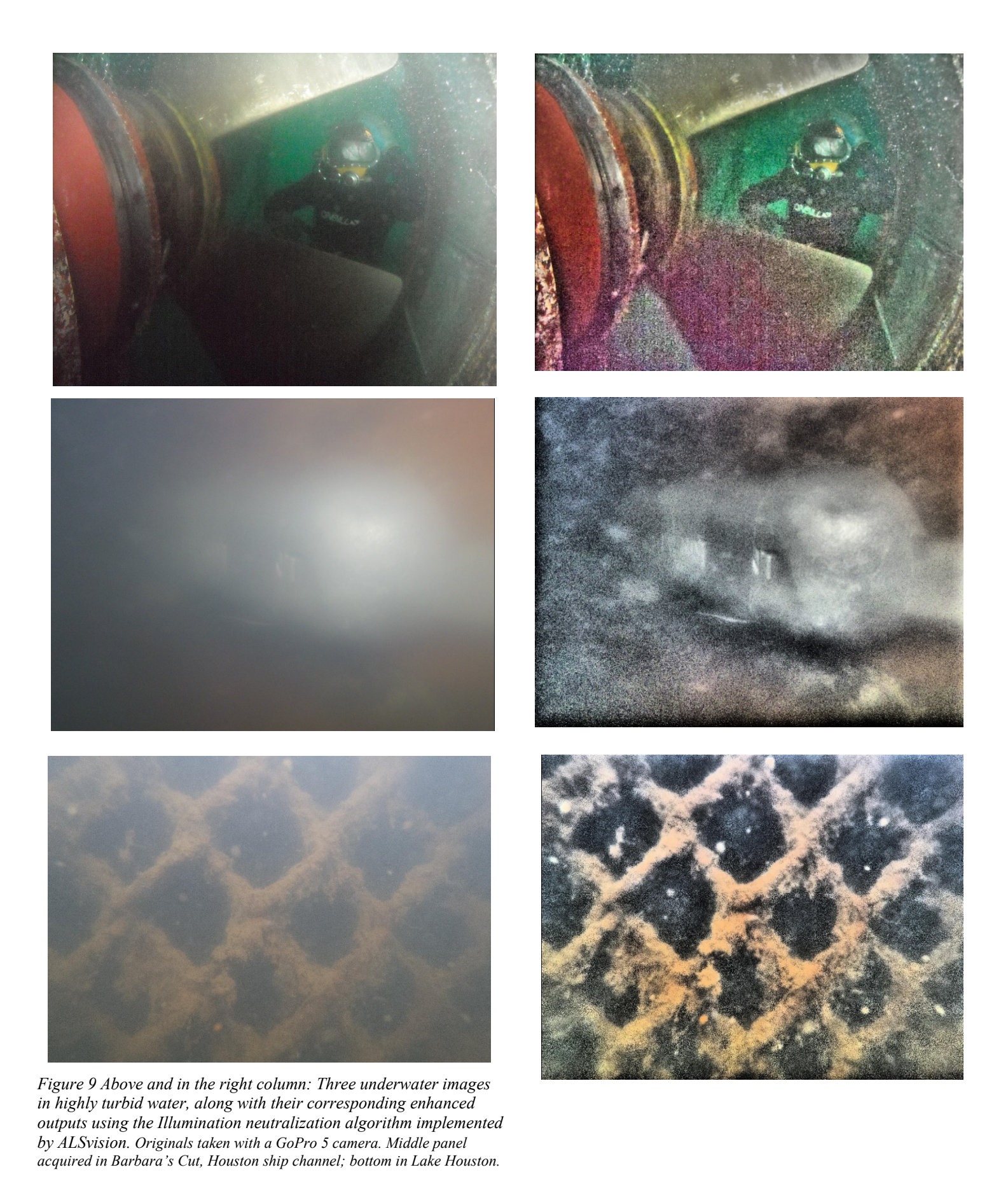
ACKNOWLEDGEMENTS

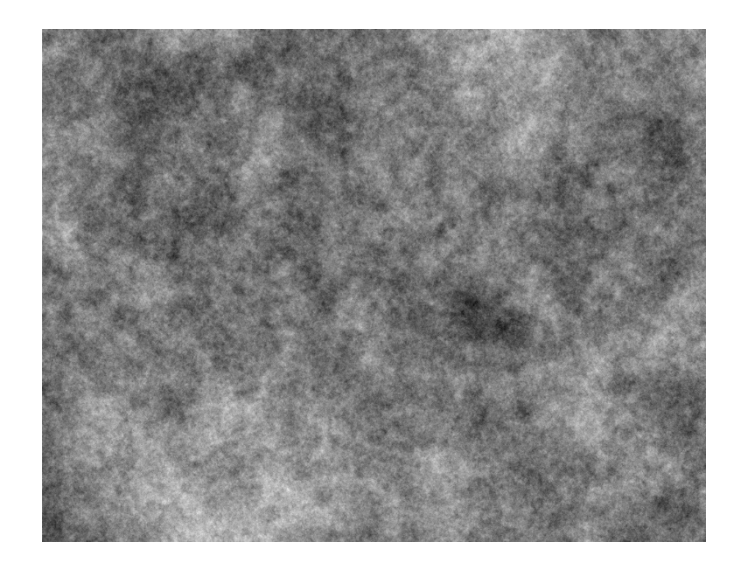
This work has been partially supported by NSF-DMS 1720487. COI Declaration: Manos Papadakis is the managing partner of Lolaark LLC in which the University of Houston is a stakeholder. Results from this work are likely to incur a financial benefit to Lolaark LLC and to UH. Papadakis' COI has been declared and monitored according to UHS policies. Underwater images used in this research were acquired by the team of Lolaark LLC. We thank Lolaark LLC for providing us data for our experiments and our partner company Texas Commercial Diving for the collection of numerous data sets as those in Fig. 9. Last, but not least, we thank the reviewer for comments that helped us to improve the presentation of our work.

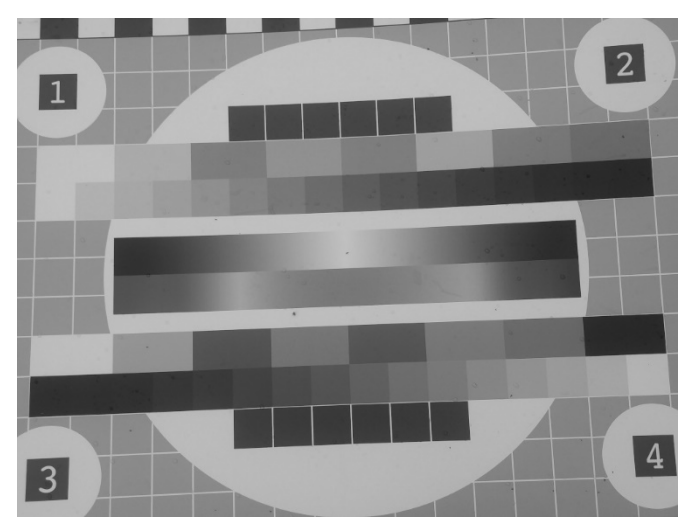
REFERENCES

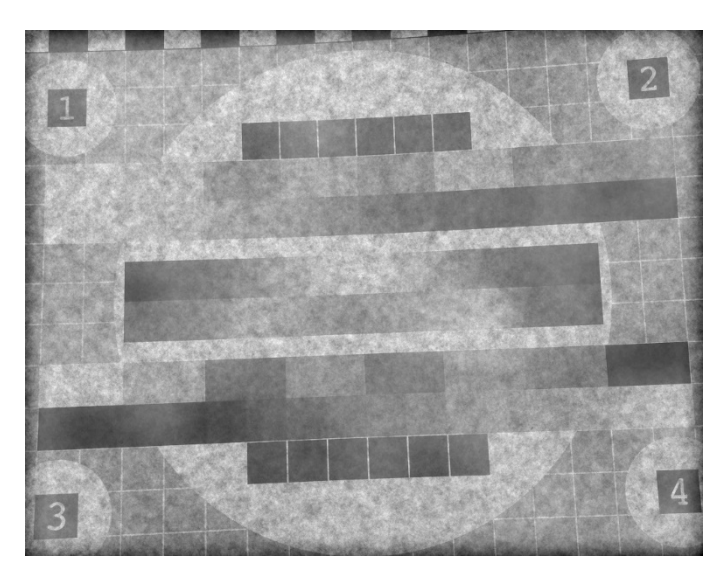
- Abry, Patrice, and Fabrice Sellan. 1996. "The wavelet-based synthesis for fractional Brownian motion proposed by F. Sellan and Y. Meyer: Remarks and fast implementation." *Applied Computational and Harrmonic Analysis* 377-383.
- Arici, T., S. Dikbas, and Y. Altunbasak. 2009. "histogram modification framework and its application for image contrast enhancement." *IEEE Transactions on Image Processing* 1921-1935.
- Brouste, Alexandre, Jacques Istas, and Sophie Lambert-Lacroix. 2007. "On fractional Gaussian random field simulations." *J. of Statistical Software* Open Access.
- Celik, T., and T. Tjahjadi. 2011. "Contextual and variational contrast enhancement." *IEEE Transactions on Image Processing* 3431-3441.
- Chiang, John, and Ying-Ching Chen. 2011. "Underwater image enhancement by wavelength compensation and dehazing." *IEEE Transactions on Image Processing* 1756-1769.

- Ding, Xueyan, Yafei Wang, Yang Yan, Zheng Linag, Zetian Mi, and Xianping Fu. 2019. "Jointly adversarial network to wavelength compensation and dehazing of underwater images."
- Fournier, Alain, Don Fussel, and Loren Carpenter. 1982. "Computer rendering of stochastic models." *Communications ACM* 371-384.
- Jaffe, S. Jules. 1990. "Computer modeling and the design of optimal underwater imaging systems." *IEEE Journal of Oceanic Engineering*, 101-111.
- Karatzas, I. and Shreve, S. 1997. *Brownian Motion and Stochastic Calculus, 2nd ed.* New York: Springer-Verlag.
- Li, Chong-Yi, Ji-Chang Guo, Run-Min Cong, Yan-Wei Pang, and Bo Wang. 2016. "Underwater image enhancement by dehazing with minimum information loss and histogram distribution prior." *IEEE Transactions on Image Processing* 5664-5677.
- Lu, Huimin, Yujie Li, Shota Nakashima, and Seiichi Serikawa. 2016. "Turbidity underwater image restoration using spectral properties." *IEICE Trans. on Information and Systems* 219-227.
- McGlamery, B.L. 1980. "A computer model for underwater camera systems." *Ocean Optics VI.* International Society for Optics and Photonics. 221-231.
- Mitsakos, Nikolaos, Sanat Upadhyay, and Manos Papadakis. 2019. Virtual Multimodal Automated Object Detection with Deep Neural Networks. Accessed 6 8, 2020. https://onepetro.org/conference-paper/sname-tos-2019-016.
- Sanat, Upadhyay., Nikolaos Mitsakos, and Manos Papadakis. 2018. "Real time visibility improvement for underwater video." *SNAME 23rd Offshore Symposium*. Houston, TX: SNAME.
- Schettini, Raimondo, and Silvia Corchs. 2010. "Underwater image processing: state of the art of restoration and image enhancement methods." *EURASIP Journal on Advances in Signal Processing* 746052.
- Upadhyay, Sanat, and Manos Papadakis. 2019. "Lifting the veil: enhancing images in turbid aqueous environments." *Wavelets and Sparsity XVIII, Optics and Photonics* 2019. San Diego, CA: SPIE. 111380W.
- Zhang, Shu, Ting Wang, Junyu Dong, and Hui Yu. 2017.
 "Underwater image enhancement via extended multiscale Retinex." *Neurocomputing* 1-9.
- Zuiderveld, Karel. 1994. "Contrast Limited Adaptive Histogram Equalization." In *Graphics Gems IV*, 474-485. San Diego CA: Academic Press Professional Inc.













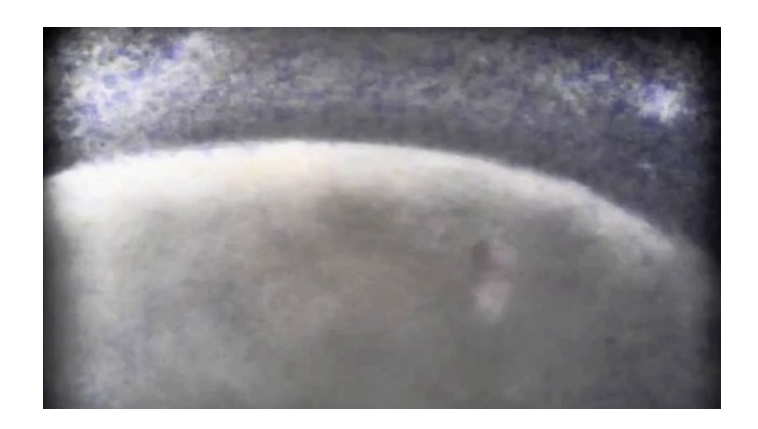


Figure 10 (Left column) The top panel shows a turbidity texture. The mid panel shows a TV-test pattern. We observe that weak edges are completely blurred by the texture, while stronger edges are mostly preserved.

Right column: Top panel: An original frame extracted from a tunnel thruster camera inspection of a M/T in turbid water (horizontal visibility around 3ft). There is a nick on the blade which is quite visible on the bottom panel generated by ALSvision. The mid panel was processed with CLAHE. Original courtesy of G&G Marine of Houston TX.









Figure 12 Top panel original captured by a pipe inspection camera, 480p (horizontal visibility around 10''). The bottom panel was generated by ALSvision. The mid panel was processed with CLAHE.

Figure 11 Original (top) shot during a rainstorm on I-10 East of Houston, TX while driving. The bottom panel shows the enhancement. The average brightness of the cloudy sky and of the road are the same since we perform illumination neutralization and not contrast enhancement.